

Light trapping and electrical transport in thin-film solar cells with randomly rough textures

Piotr Kowalczewski, Angelo Bozzola, Marco Liscidini, and Lucio Claudio Andreani

Citation: *Journal of Applied Physics* **115**, 194504 (2014); doi: 10.1063/1.4876223

View online: <http://dx.doi.org/10.1063/1.4876223>

View Table of Contents: <http://scitation.aip.org/content/aip/journal/jap/115/19?ver=pdfcov>

Published by the [AIP Publishing](#)

Articles you may be interested in

[Towards high efficiency thin-film crystalline silicon solar cells: The roles of light trapping and non-radiative recombinations](#)

J. Appl. Phys. **115**, 094501 (2014); 10.1063/1.4867008

[Modulated surface textures for enhanced light trapping in thin-film silicon solar cells](#)

Appl. Phys. Lett. **97**, 101106 (2010); 10.1063/1.3488023

[Impact of front and rear texture of thin-film microcrystalline silicon solar cells on their light trapping properties](#)

J. Appl. Phys. **108**, 044505 (2010); 10.1063/1.3467968

[Effect of self-orderly textured back reflectors on light trapping in thin-film microcrystalline silicon solar cells](#)

J. Appl. Phys. **105**, 094511 (2009); 10.1063/1.3108689

[Local versus global absorption in thin-film solar cells with randomly textured surfaces](#)

Appl. Phys. Lett. **93**, 061105 (2008); 10.1063/1.2965117



HIDEN
ANALYTICAL

Instruments for Advanced Science

 <p>Gas Analysis</p> <ul style="list-style-type: none">dynamic measurement of reaction gas streamscatalysis and thermal analysismolecular beam studiesdissolved species probesfermentation, environmental and ecological studies	 <p>Surface Science</p> <ul style="list-style-type: none">UHV TPDSIMSend point detection in ion beam etchelemental imaging - surface mapping	 <p>Plasma Diagnostics</p> <ul style="list-style-type: none">plasma source characterizationetch and deposition process reactionkinetic studiesanalysis of neutral and radical species	 <p>Vacuum Analysis</p> <ul style="list-style-type: none">partial pressure measurement and control of process gasesreactive sputter process controlvacuum diagnosticsvacuum coating process monitoring
--	---	---	---

Contact Hiden Analytical for further details:
W www.HidenAnalytical.com
E info@hiden.co.uk
CLICK TO VIEW our product catalogue

Light trapping and electrical transport in thin-film solar cells with randomly rough textures

Piotr Kowalczewski,^{a)} Angelo Bozzola, Marco Liscidini, and Lucio Claudio Andreani
Department of Physics and CNISM, University of Pavia, Via Bassi 6, I-27100 Pavia, Italy

(Received 21 March 2014; accepted 30 April 2014; published online 20 May 2014)

Using rigorous electro-optical calculations, we predict a significant efficiency enhancement in thin-film crystalline silicon (c-Si) solar cells with rough interfaces. We show that an optimized rough texture allows one to reach the Lambertian limit of absorption in a wide absorber thickness range from 1 to 100 μm . The improvement of efficiency due to the roughness is particularly substantial for thin cells, for which light trapping is crucial. We consider Auger, Shockley-Read-Hall (SRH), and surface recombination, quantifying the importance of specific loss mechanisms. When the cell performance is limited by intrinsic Auger recombination, the efficiency of 24.4% corresponding to the wafer-based PERL cell can be achieved even if the absorber thickness is reduced from 260 to 10 μm . For cells with material imperfections, defect-based SRH recombination contributes to the opposite trends of short-circuit current and open-circuit voltage as a function of the absorber thickness. By investigating a wide range of SRH parameters, we determine an optimal absorber thickness as a function of material quality. Finally, we show that the efficiency enhancement in textured cells persists also in the presence of surface recombination. Indeed, in our design the efficiency is limited by recombination at the rear (silicon absorber/back reflector) interface, and therefore it is possible to engineer the front surface to a large extent without compromising on efficiency. © 2014 AIP Publishing LLC. [<http://dx.doi.org/10.1063/1.4876223>]

I. INTRODUCTION

Thin-film solar cells may have significant advantages over conventional thick cells, including lower bulk transport losses, higher open-circuit voltage V_{OC} , reduced cost, and shorter fabrication time.¹ Yet, the central problem of thin-film photovoltaics is to capture and absorb sunlight in a thin active layer. In this regard, light-trapping strategies have to be both effective and not detrimental to the electrical transport.² This remains a challenging task, and therefore thin-film solar cells still struggle to compete with standard wafer-based devices in terms of energy conversion efficiency.

If one considers only the optical properties of the cell, the absorption obtained for a perfectly diffusive (Lambertian) scatterer is often taken as the theoretical limit.^{3,4} Yet, the question of what is an optimal light-trapping scheme remains open, and many strategies have been investigated, including plasmonic nanoparticles⁵⁻⁷ and photonic structures with different levels of disorder.⁸⁻¹⁷ Some of the light-trapping schemes reported so far show excellent absorption close to or even beyond the Lambertian limit.¹⁸⁻²¹ Moreover, structures reaching the Lambertian limit have also been demonstrated experimentally.^{22,23}

These light-trapping strategies are usually evaluated assuming that each absorbed photon contributes to the photocurrent. Therefore, the corresponding short-circuit current and efficiency are calculated without considering the electrical losses. Yet, light-trapping schemes may substantially affect the electrical properties of the cell.²⁴⁻²⁹

Among many light-trapping strategies, random textures³⁰⁻³⁷ are particularly useful for photovoltaic applications as intrinsically broadband scatterers. In this work, we use rigorous electro-optical calculations to study the performance of randomly rough crystalline silicon (c-Si) solar cells with the absorber thickness ranging from 1 to 100 μm . Recent advances in laser crystallization of thin silicon films,³⁸ as well as epitaxial³⁹ and epitaxy-free⁴⁰⁻⁴² fabrication of micron-scale c-Si films justify this choice of the material. Moreover, c-Si solar cells do not suffer from poor material quality, which is a considerable weakness of solar cells made of microcrystalline ($\mu\text{c-Si}$) or amorphous (a-Si) silicon.⁴³⁻⁴⁵

In our approach, we take advantage of the isotropy of the considered rough textures in the optical as well as electrical calculations. The simulated structures are two-dimensional, but the results are generalized to three-dimensional systems with a simple rescaling procedure. By doing so we are able to investigate a wide range of material parameters and obtain accurate results at a significantly reduced computational cost. We model the rough interfaces as a one-dimensional Gaussian roughness, which is able to describe the optical properties of state-of-the-art rough textures, i.e., Neuchâtel and Asahi-U substrates.⁴⁶ Height histograms of these textures, including comparison with Gaussian distributions, have been documented in the literature.^{36,47}

We start by calculating the efficiency limit of randomly rough c-Si solar cells in the presence of intrinsic Auger recombination. Then, we consider the material quality of one of the most efficient thin-film c-Si solar cells reported in the literature, and we investigate the gap between the performance of state-of-the-art cells and the calculated efficiency

^{a)}piotr.kowalczewski@unipv.it

limit. Finally, we focus on surface recombination, expected to be particularly important in thin-film textured solar cells, with increased surface area and high surface-to-volume ratio. As a final result, we quantify the upper limits for bulk and surface recombination, showing that 10 μm thick c-Si solar cells with 20% energy conversion efficiency are in reach of present-day fabrication technologies.

This paper is organized as follows: Section II describes our approach to electro-optical simulations of randomly rough solar cells. This section covers the model of roughness, calculation of the photogeneration profile, and its transfer to the electrical simulator. Section III focuses on light trapping and bulk transport losses in randomly rough solar cells. Section IV shows how textured solar cells are limited by surface recombination. Conclusions are given in Sec. V.

II. NUMERICAL APPROACH

In our approach, the distribution of the electric field within a rough solar cell is calculated using Rigorous Coupled-Wave Analysis (RCWA),^{48,49} and roughness is described by the staircase approximation. We assume that the cell is illuminated at normal incidence by unpolarized light. The electric field is used to calculate the photogeneration profile,^{24–26} which then serves as an input for the device simulator. Finally, we model the solar cell performance by solving the drift-diffusion equations by means of finite-element approximation with Silvaco Atlas device simulator.⁵⁰ We consider two-dimensional structures in the optical and electrical calculations. Yet, we use the known ratio between the two-dimensional and one-dimensional Lambertian limit of absorption to rescale the photogeneration profile to the one corresponding to three-dimensional systems.

A. Model of roughness

Detailed description of our optical model and its validation can be found in our previous works.^{46,51} Here, for the sake of completeness, we only highlight the main points.

We model rough textures as a one-dimensional random roughness with Gaussian distribution of height and Gaussian correlation function, describing the lateral features of the interface. The roughness is characterized by two statistical parameters: root mean square (RMS) deviation of height σ and lateral correlation length l_c . To generate random roughness with a given σ and l_c , we use Eq. (A.27) derived in Ref. 52. The series is expanded up to $k = 151$ (the order of expansion is the same as the number of plane waves used in the RCWA calculations). Period of the computational cell is $L = 10 \mu\text{m}$, much larger than correlation length of the considered rough textures, which allows to neglect the effects of periodicity.

To validate this approach, we have calculated the optical properties, i.e., Angular Intensity Distribution and haze, of rough Gaussian interfaces with σ and l_c corresponding to two commonly used rough substrates, namely Neuchâtel and Asahi-U. Then, we compared our results with similar calculations performed for two-dimensional measured surface topographies.⁵³ This comparison gave a very good agreement, and therefore proved that this simple 1D model of Gaussian

roughness accurately describes the optical properties of 2D realistic rough topographies.⁴⁶ Such a good agreement was possible because the considered rough substrates scatter light isotropically.

B. Rescaling the photogeneration profile and electrical calculations

The electric field calculated for a two-dimensional structure is used to obtain the photogeneration rate, namely the number of photo-generated electron-hole pairs per unit area and unit time as a function of position. First, we calculate the absorption rate as

$$a(x, z, E) = \varepsilon_2(E) \frac{2\pi E}{hc} \frac{|\mathcal{E}(x, z, E)|^2}{|\mathcal{E}_{\text{inc}}(E)|^2}, \quad (1)$$

where ε_2 is the imaginary part of the dielectric function of c-Si,⁵⁴ E is the energy of photon, c is the speed of light in vacuum, h is Planck constant, $\mathcal{E}(x, z, E)$ is the electric field within the structure, and $\mathcal{E}_{\text{inc}}(E)$ corresponds to the incident light, assumed to be a plane wave.

The total absorption in the active layer as a function of energy can be obtained by integrating Eq. (1) over the area of silicon

$$A(E) = \int_{Si} a(x, z, E) dx dz, \quad (2)$$

whereas the position-dependent photogeneration rate can be calculated as

$$G_{\text{opt}}^{2D}(x, z) = \int \frac{I(E)}{E} a(x, z, E) dE, \quad (3)$$

where $I(E)$ is the spectral irradiance corresponding to the AM1.5G solar spectrum,⁵⁵ and the integration is done for the energy window between 1.1 and 4.2 eV, i.e., from the energy band-gap of c-Si up to the energy above which the solar photon flux is negligible.

So far, these calculations refer to a one-dimensional interface, and thus the calculated photogeneration profile corresponds to a two-dimensional solar cell. As previously shown, this one-dimensional model of rough interface can describe the optical properties of two-dimensional isotropic textures.⁴⁶ Yet, the photogeneration profile calculated for a one-dimensional roughness has to be renormalized to account for a larger number of scattering channels for a two-dimensional interface. Such a renormalization is based on the analogy between randomly rough textures and the theoretical Lambertian scatterer,³ describing a perfectly scattering (diffusive) interface. Indeed, an optimized rough texture reproduces the absorption spectrum of the Lambertian limit, and the total absorption in the rough active layer is more than 94% of the absorption provided by the Lambertian scatterer.⁵¹ Thus, we can introduce a rescaling factor, namely the ratio of the absorption in the structure with the 2D Lambertian scatterer to the absorption corresponding to the 1D Lambertian scatterer.^{3,18} This, for a given absorber thickness d , can be written as

$$C_d(E) = \frac{A_{LL}^{2D}(E)}{A_{LL}^{1D}(E)}. \quad (4)$$

In Fig. 1, we plot the rescaling factor C_d as a function of energy for the absorber thickness range considered in this work. For small energies and thin cells, the factor is proportional to $4n^2/(\pi n)$, where n is the refractive index of silicon. For high energies, where silicon absorbs very well, the factor approaches unity. The trends for different absorber thickness are similar, but the values of the rescaling factor are higher for thinner cells.

In our calculations, we assume that for a given energy and thickness of the absorber, the rescaling factor is independent of the position (x,z) . This assumption is supported by the results shown in Fig. 2, where we plot the absorption rate as a function of depth at four different energies, calculated for $1\ \mu\text{m}$ thick silicon absorbers with the 1D and 2D Lambertian scatterer.

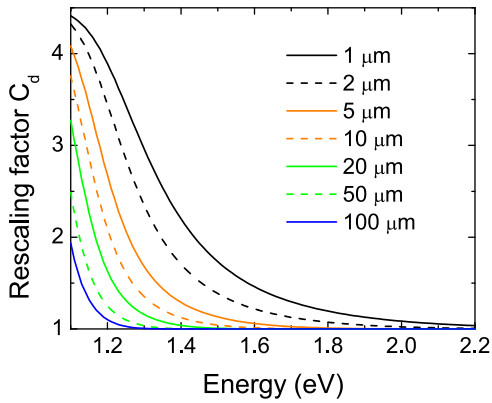


FIG. 1. Rescaling factor used to calculate the photogeneration profile corresponding to two-dimensional rough textures, based on calculations of a one-dimensional roughness. The factor is defined as the ratio of the absorption obtained for the 2D Lambertian scatterer to the absorption corresponding to the 1D Lambertian scatterer.

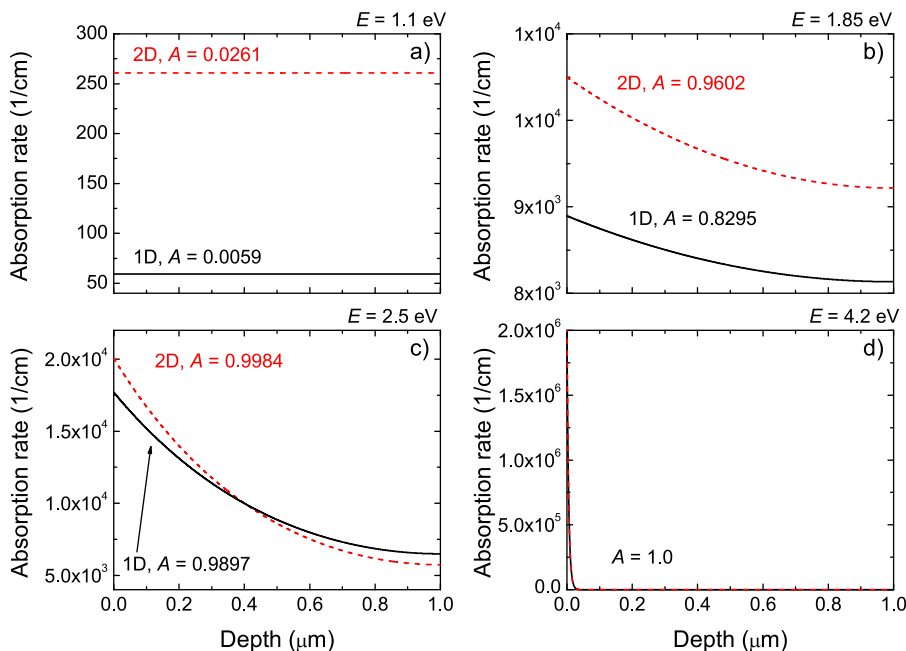


FIG. 2. Absorption rate as a function of depth at four different energies, calculated for $1\ \mu\text{m}$ thick silicon absorbers with the 1D and 2D Lambertian scatterer.

Finally, the photogeneration rate corresponding to a three-dimensional solar cell is calculated as

$$G_{\text{opt}}^{3D}(x, z) = \int C_d(E) \frac{I(E)}{E} a(x, z, E) dE. \quad (5)$$

The photogeneration profile calculated with Eq. (5) is projected onto a finite-element mesh and serves as an input for the device simulator,⁵⁰ which models the solar cell performance by solving the drift-diffusion equations. To avoid the dependence on a particular rough surface realization, the results are averaged over 10 solar cell structures, each with a different surface realization.

For each analysed solar cell structure and surface realization, we verify the photogeneration profile transfer and accuracy of the mesh in the device simulator. This is done by using the photogeneration profile before rescaling, obtained with Eq. (3), to calculate the short-circuit current density J_{sc}^{2D} in the limit of no recombination losses, i.e., reproducing the state of unity electron-hole pair collection efficiency. In this case, the expected short-circuit current density is given by¹

$$J_{\text{sc}}^{\text{opt}} = q \int \frac{I(E)}{E} A(E) dE, \quad (6)$$

where $A(E)$ is the total absorption in the active layer calculated with RCWA. We impose that J_{sc}^{2D} obtained with the device simulator cannot differ by more than 1% from $J_{\text{sc}}^{\text{opt}}$.

III. LIGHT TRAPPING AND BULK TRANSPORT LOSSES

The investigated structure is sketched in Fig. 3(a). It consists of a crystalline silicon⁵⁴ absorber with an anti-reflection coating (ARC) and a silver⁵⁴ back reflector. The volume of silicon is kept constant for different parameters of the roughness, and it corresponds to a flat absorber with thickness d . The 70 nm thick ARC is transparent with

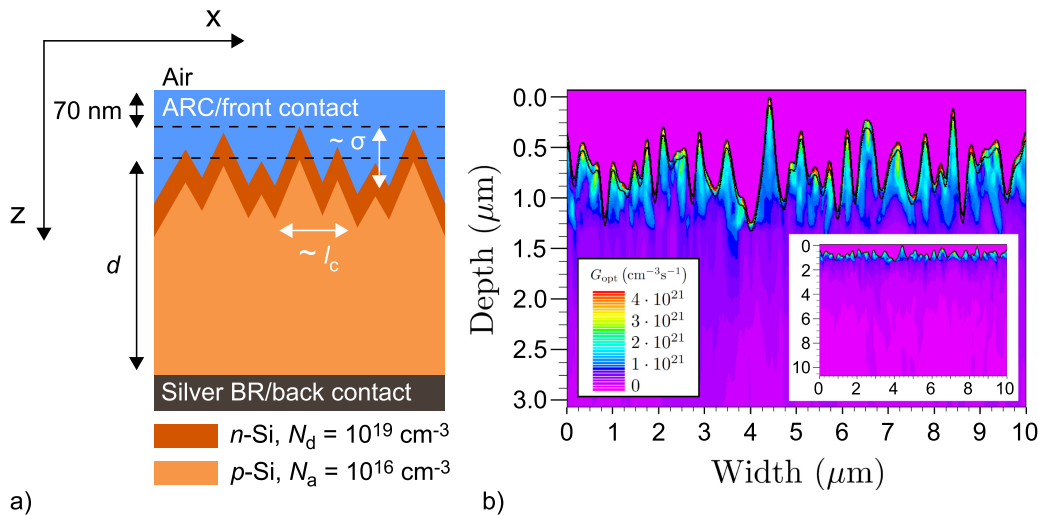


FIG. 3. (a) Investigated solar cell structure, consisting of crystalline silicon absorber, ARC, silver back reflector, and randomly rough texture. The roughness is characterized by root mean square deviation of height σ and lateral correlation length l_c . The p - n junction is made of an 80 nm thick n -type layer (emitter) with donor concentration $N_d = 10^{19} \text{ cm}^{-3}$, and p -type layer (base) with acceptor concentration $N_a = 10^{16} \text{ cm}^{-3}$. (b) Example of the photogeneration profile calculated for the 10 μm thick c -Si solar cell. Black lines at the top of the roughness indicate the junction. The main plot shows the photogeneration profile close to the texture, whereas the inset shows the whole cell. Lengths in the inset are given in μm .

refractive index $n = 1.65$. We consider a p - n junction made of an 80 nm thick n -type layer with donor concentration $N_d = 10^{19} \text{ cm}^{-3}$, and p -type layer with acceptor concentration $N_a = 10^{16} \text{ cm}^{-3}$.¹ Finally, the parameters of the simulated Gaussian texture are the optimal values for c -Si: $\sigma = 300 \text{ nm}$ and $l_c = 160 \text{ nm}$.⁴⁶ To put these values into perspective with realistic rough topographies, we note that (1) with increasing σ , photocurrent saturates,^{46,53} and the saturation value of σ depends on l_c , e.g., for $l_c = 160 \text{ nm}$ photocurrent saturates at $\sigma \approx 200 \text{ nm}$; (2) for a given σ , photocurrent as a function of l_c exhibits a wide maximum (i.e., photocurrent mainly depends on σ , with a modest, bell-like dependence on l_c).^{46,51} For these reasons, performance similar to that of the Gaussian roughness can be achieved for realistic rough textures with different feature sizes and more moderate aspect ratios, preferred in practical devices.^{39,56}

In Fig. 3(b), we show an example of the photogeneration profile, calculated for the 10 μm thick solar cell. The photogeneration profile is calculated for the energy window between 1.1 and 4.2 eV, and averaged over both polarizations. We note that no mode pattern is present, implying that the photogeneration profile is mainly due to the light scattering, without any appreciable contribution from the guided modes of the film. This is significantly different from structures with ordered or partially disordered photonic crystals, where the light-trapping mechanism is based on coupling of the incident light into the guided modes, and the mode pattern in the photogeneration profile should be recognized.

In Fig. 4, we show calculated efficiency η , short-circuit current density J_{sc} , fill factor (FF), and open-circuit voltage V_{oc} as a function of thickness for flat and randomly rough solar cells. We consider structures limited by intrinsic Auger recombination, as well as cells with material imperfections resulting in Shockley-Read-Hall (SRH) recombination. At this point, we assume no surface recombination.

The Auger coefficients in p -type and n -type layers are $C_p = 9.9 \times 10^{-32} \text{ cm}^6 \text{ s}^{-1}$ and $C_n = 2.8 \times 10^{-31} \text{ cm}^6 \text{ s}^{-1}$,

respectively.⁵⁸ For SRH recombination, the diffusion length of electrons in the p -type layer is $L_n = 232 \mu\text{m}$, which corresponds to one of the most efficient thin-film c -Si solar cells.³⁹ The difference is that the value of L_n reported in Ref. 39 is an effective diffusion length, whereas in this work we assign it to SRH recombination, treating Auger recombination separately. To account for a poor carrier collection efficiency in the highly doped n -type layer, we assume the diffusion length of holes in the emitter L_p to be 10 times smaller than L_n ,¹ therefore $L_p = 23.2 \mu\text{m}$.

Figure 4(a) shows a significant efficiency enhancement due to the surface texturing. The improvement is particularly substantial for thinner cells, for which light trapping is crucial. For example, the efficiency of the 1 μm thick rough solar cell in absolute units is 8.9% (Auger only) and 7.7% (Auger + SRH) higher than the efficiency of the corresponding flat cell. The results for cells limited by Auger recombination can be compared with the efficiency of the wafer-based 260 μm thick PERL cell,⁵⁷ showing that the same energy conversion efficiency can be achieved for rough c -Si cells with the active layer as thin as 10 μm .

Both FF and V_{oc} are just slightly modified by the roughness, as shown in Figs. 4(c) and 4(d). Thus, the observed efficiency enhancement for rough solar cells can be easily attributed to a much higher short-circuit current density, shown in Fig. 4(b). Indeed, J_{sc} in textured cells can reach more than 94% of the Lambertian limit regardless of the thickness of the active layer (reflection losses at the air/ARC interface have been included in the Lambertian limit). Absorption in thicker cells is even closer to the Lambertian limit, because parasitic losses in the silver back reflector become less important with increasing thickness of the absorber. We note that the optimal parameters of the roughness do not depend on the absorber thickness. This is very different from cells with diffraction gratings and photonic crystals, where light trapping is based on interference in the active layer, and thus optimal parameters of the texture strongly depend on the absorber thickness. This

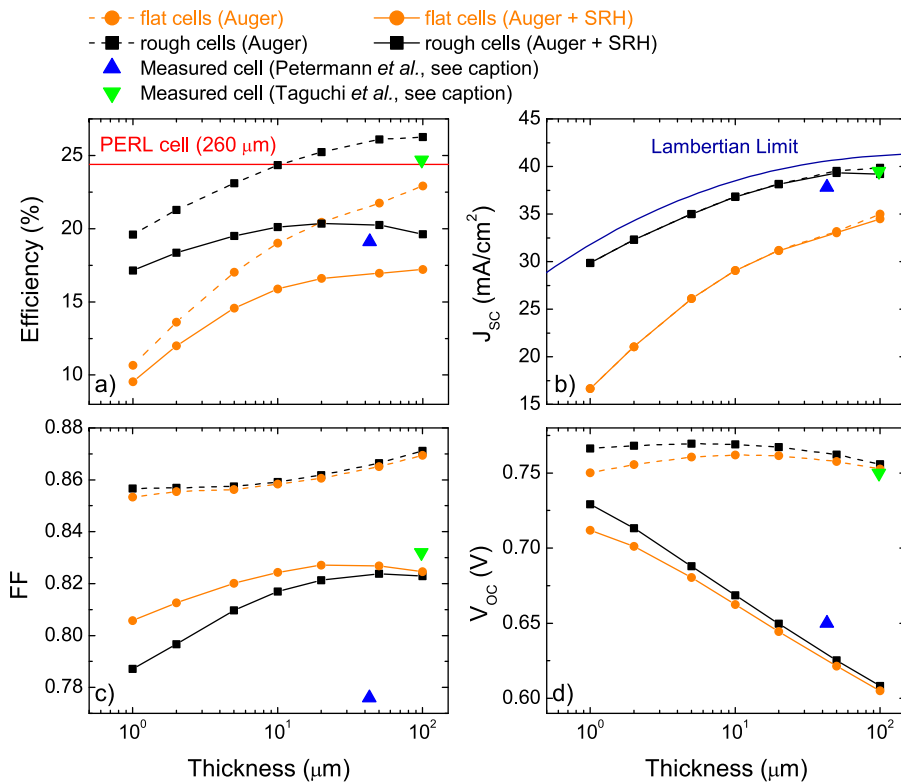


FIG. 4. (a) Efficiency, (b) short-circuit current J_{sc} , (c) FF, and (d) open-circuit voltage V_{oc} as a function of the absorber thickness for flat and textured solar cells. Efficiency is compared with the performance of the wafer-based 260 μm thick PERL cell.⁵⁷ J_{sc} is compared with the corresponding Lambertian limit. We consider structures limited by intrinsic Auger recombination, as well as cells with material imperfections resulting in SRH recombination. At this point, we assume no surface recombination. The parameters of the rough texture are the optimal values for c-Si: $\sigma = 300 \text{ nm}$ and $l_c = 160 \text{ nm}$.⁴⁶ The blue and green triangles indicate the values corresponding to, respectively, the 43 μm thick³⁹ and 98 μm thick⁵⁶ randomly textured c-Si solar cells, used as benchmark structures.

difference in light-trapping mechanisms makes the design based on rough textures especially robust.

When the effects of SRH recombination are taken into account, thinner solar cells may be more efficient than thicker ones. An optimal absorber thickness depends on material quality and results from the opposite trends of short-circuit current and open-circuit voltage as a function of the cell thickness, as shown in Figs. 4(b) and 4(d). This conclusion is consistent with our previous work, proposing an analytical model to study the role of light trapping and non-radiative recombination in solar cells.⁵⁹

SRH recombination mainly impacts on V_{oc} , leaving J_{sc} practically unaffected. We attribute this behaviour to the assumed material quality, for which the diffusion lengths of the minority carriers in the emitter and in the base are larger than thickness of the corresponding layer, keeping the internal quantum efficiency high. The voltage drop due to SRH recombination is particularly large for thick cells, more sensitive to bulk recombination.

Finally, in Fig. 4(c) we show that when SRH recombination is considered, flat cells exhibit higher FF than rough structures. We believe this is due to the increased area of the junction, which causes FF drop in the presence of SRH recombination.

The blue triangles in Fig. 4 indicate the values corresponding to the 43 μm thick randomly textured c-Si solar cell, fabricated by epitaxial growth using porous silicon.³⁹ With 19.1% efficiency, it is one of the most efficient thin-film c-Si solar cells reported in the literature. In our simulations, we used the same bulk material quality, which allows us to consider this cell as a reference to assess our numerical results. The reference and simulated cells exhibit similar efficiencies and currents. The differences in V_{oc} may be attributed to different junction parameters, such as junction depth

or doping profile. Fill factor is mainly influenced by series resistance of the contacts and shunt resistance related to the manufacturing imperfections. These effects are not taken into account in our model, and thus the calculations are likely to slightly overestimate the fill factor.

Recently reported 98 μm thick heterojunction with intrinsic thin-layer (HIT) c-Si solar cell with an excellent efficiency of 24.7% (Ref. 56) may serve as another benchmark structure. The performance of this cell is indicated with the green triangles in Fig. 4. In this case, the measured values of V_{oc} and J_{sc} are similar to those corresponding to the simulated structure limited by Auger recombination. Yet, as discussed above, the model may slightly overestimate the fill factor.

As already noticed, when the absorber becomes too thick, the voltage losses caused by SRH recombination exceed the current gain. The question is, how does an optimal thickness of the absorber depend on material quality? In our design, the emitter is much thinner than the base, thus the cell performance is likely to be limited by the diffusion length L_n of electrons in the base. In Fig. 5, we show efficiency as a function of L_n and the absorber thickness. As expected, thicker cells are more sensitive to the bulk losses; for a poor material quality, i.e., for diffusion-limited solar cells, increasing the absorber thickness almost immediately decreases the efficiency. Yet, an optimal thickness shifts towards thicker cells with increasing material quality.

IV. SURFACE RECOMBINATION

In the results presented so far, we have considered only bulk losses, neglecting surface recombination. Yet, the direct consequence of texturing the absorber layer is increased

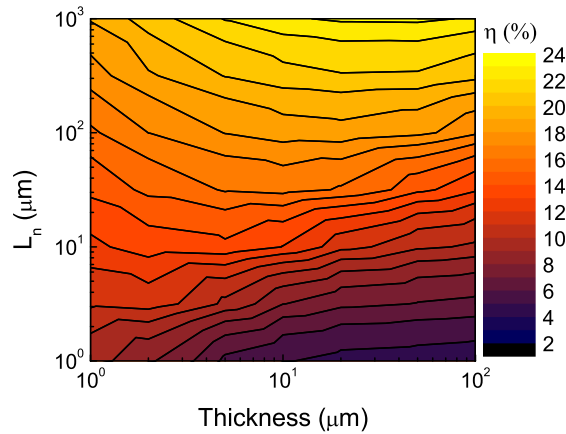


FIG. 5. Efficiency as a function of diffusion length of electrons in the base L_n and the absorber thickness. As in the previous calculations, diffusion length of holes in the emitter is $L_p = 23.2 \mu\text{m}$.

front surface area. Therefore, one may expect that surface recombination is an important factor limiting the performance of solar cells, especially in the case of thin textured cells, with a large surface-to-volume ratio.

In Fig. 6, we show efficiency as a function of top and bottom surface recombination velocity (SRV) calculated for the $10 \mu\text{m}$ thick c-Si solar cell. These results indicate that the efficiency is limited by recombination at the rear interface, and for front SRV below 10^4 cm/s the impact of surface recombination on the cell performance is negligible (i.e., the efficiency drops by less than 1% in relative units). This result can be generalized to different thickness, although thinner cells tend to be more sensitive to surface recombination, e.g., for the $1 \mu\text{m}$ thick cell, the efficiency drops by 1% (relative units) for top SRV higher than 10^3 cm/s .

The conclusion that recombination at the rear surface is more important than that at the front surface has an intuitive physical explanation: Only the minority carriers are sensitive to recombination losses. Therefore, the importance of surface recombination at a given surface depends on the amount of minority carriers in the layer close to this surface. In our design, the n -type emitter is only 80 nm thick, thus most of the light is absorbed in the base, and therefore

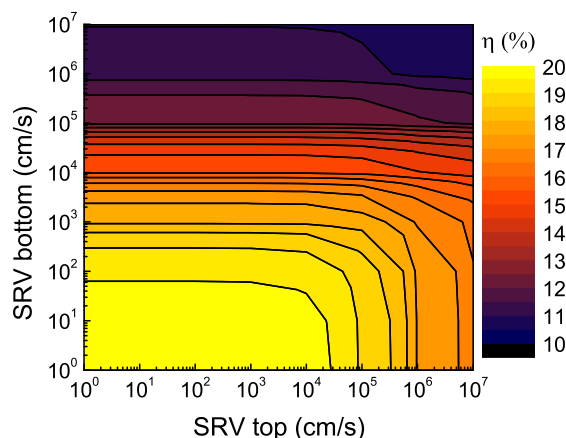


FIG. 6. Efficiency as a function of top and bottom SRV for the $10 \mu\text{m}$ thick c-Si solar cell. SRH recombination with $L_n = 232 \mu\text{m}$ and $L_p = 23.2 \mu\text{m}$ is included.

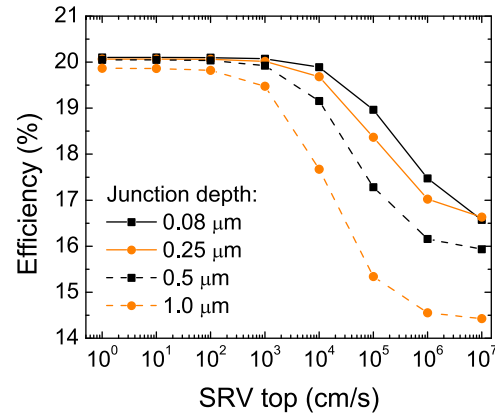


FIG. 7. Efficiency as a function of top SRV for different junction depths, calculated for the $10 \mu\text{m}$ thick rough c-Si solar cell. Bottom SRV is assumed to be 1 cm/s . SRH recombination with $L_n = 232 \mu\text{m}$ and $L_p = 23.2 \mu\text{m}$ is included.

the minority carriers are mainly in the much thicker p -type layer.

Since the amount of minority carriers in a given layer is directly related to the absorption in this layer, the upper limit for surface recombination may depend not only on the layer thickness but also on absorption coefficient and configuration of the solar cell structure (e.g., the situation may be different in p - i - n configuration, typical for a-Si solar cells).

To support this explanation, in Fig. 7 we plot the efficiency as a function of top SRV for different junction depths. Here, we focus only on the front surface and assume $\text{SRV}_{\text{bottom}} = 1 \text{ cm/s}$. These results show that the front surface recombination becomes more important with increasing junction depth, which is in agreement with the reasoning presented above. The drop of the efficiency for $\text{SRV}_{\text{top}} = 1 \text{ cm/s}$ is due to bulk recombination.

This analysis predicts that, as far as surface recombination is concerned, it is possible to engineer the front surface to a large extent without compromising on efficiency. We note, however, that efficiency of a textured cell may be limited by other technological imperfections, such as microvoids observed in layers deposited on rough substrates.^{44,60} While these practical limitations are beyond the scope of the present paper, we notice that problems associated to roughness with large RMS height σ can be mitigated by a hybrid structure that combines moderate roughness with a photonic crystal.⁵¹

We also note that in this work we focus on carrier recombination at the textured front interface, and therefore in the considered solar cell structure we do not include additional elements to reduce rear-side recombination, such as passivation layer or back surface field, commonly used in realistic devices.¹

Finally, another question concerns the interplay between bulk and surface recombination. In Fig. 8, we show the cell efficiency as a function of diffusion length L_n and (a) top SRV, (b) bottom SRV. In both cases, the cell performance is more sensitive to surface recombination for a higher bulk material quality (with bottom SRV more important than top SRV, as shown previously). In other words, if the maximum possible efficiency is reduced by a poor bulk material

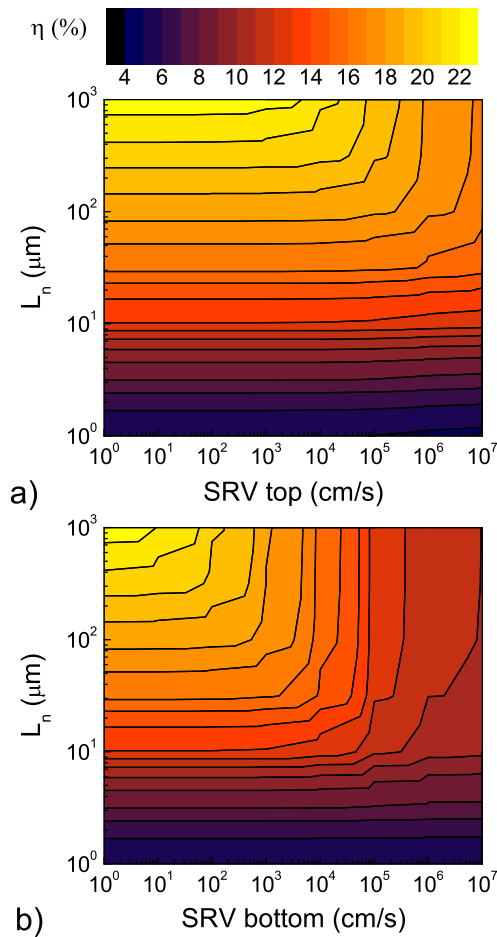


FIG. 8. Efficiency as a function of diffusion length of electrons in the base L_n and (a) top and (b) bottom SRV, calculated for the $10\ \mu\text{m}$ thick c-Si solar cell.

quality, the conditions for reaching this efficiency are relaxed. In the less favourable cases, when the bulk quality is very bad, surface recombination does not matter anymore; minority carriers recombine in the bulk before they can get to the surface.

V. CONCLUSIONS

We have combined optical calculations (RCWA) and electrical calculations (Silvaco Atlas device simulator) to perform a comprehensive electro-optical analysis of rough c-Si solar cells. Both in the optical and electrical calculations, we considered two-dimensional structures with complete randomly rough topography. Yet, isotropy of the rough textures allowed us to generalize the results to three-dimensional systems. By doing so, we were able to efficiently investigate a wide range of material parameters, and obtain accurate results at a significantly reduced computational cost.

We have shown that an optimized rough texture allows one to reach the Lambertian limit of absorption in the cells with the absorber thickness ranging from 1 to $100\ \mu\text{m}$. The optimal parameters of the Gaussian roughness ($\sigma = 300\ \text{nm}$, $l_c = 160\ \text{nm}$) do not depend on the absorber thickness. Thus, light-trapping schemes based on rough textures are more robust comparing to those based on gratings and photonic crystals, which perform well in the lower end of the absorber

thickness range. We also note that in realistic structures, random pyramids with a lower aspect ratio can perform equally well in the upper end of the thickness range.

We have predicted a significant efficiency enhancement due to the broadband light trapping provided by the roughness. This improvement is especially strong for thin cells. In particular, for the $1\ \mu\text{m}$ thick solar cell with a realistic bulk material quality, the efficiency is nearly 8% (absolute units) higher with respect to the flat cell. This excellent performance of rough c-Si solar cells persists also in the presence of surface recombination. Indeed, in our design the cell efficiency is limited by recombination at the rear (silicon absorber/back reflector) interface, and therefore it is possible to engineer the front surface to a large extent without compromising on efficiency. This is because the n -type emitter, close to the front surface, is much thinner than the base. Therefore, most of the light is absorbed in the p -type layer, and the minority carriers (sensitive to bulk and surface recombination) are mainly in the base.

Our analysis shows that if bulk material quality corresponds to one of the most efficient thin-film c-Si solar cells reported in the literature, and front surface recombination velocity is below $10^4\ \text{cm/s}$, it is possible to achieve 20% efficiency for solar cells as thin as $10\ \mu\text{m}$. We note that present-day passivation techniques allow much smaller SRV.⁶¹

We emphasize that our main motivation to study thin-film solar cells is to obtain efficiency comparable or even higher than that of thick cells. Indeed, the opposite trends of short-circuit current and open-circuit voltage as a function of thickness result in an optimal absorber thickness of the order of tens of micrometers, except for very high quality solar cells limited by Auger recombination, for which an optimal thickness approaches the bulk values. Thus, quantifying the conditions for which thin-film solar cells can be more efficient than bulk ones is an important result towards the development of new generation c-Si solar cells.

ACKNOWLEDGMENTS

This work was supported by the EU through Marie Curie Action FP7-PEOPLE-2010-ITN Project No. 264687 “PROPHET.” We also acknowledge CINECA/CASPUR project “Disorder” under the ISCRA initiative, for the availability of high performance computing resources and support. The authors are grateful to Francesco Buatier de Mongeot for helpful suggestions. P.K. would like to acknowledge Valeria Cinnera and Salvatore Rinaudo from ST Microelectronics (Catania Site) for the advanced training in Silvaco Atlas simulator.

¹J. Nelson, *The Physics of Solar Cells* (Imperial College Press, London, 2003).

²F. Priolo, T. Gregorkiewicz, M. Galli, and T. F. Krauss, *Nat. Nanotechnol.* **9**, 19 (2014).

³M. A. Green, *Prog. Photovoltaics* **10**, 235 (2002).

⁴E. Yablonovitch, *J. Opt. Soc. Am.* **72**, 899 (1982).

⁵S. Morawiec, M. J. Mendes, S. Mirabella, F. Simone, F. Priolo, and I. Crupi, *Nanotechnology* **24**, 265601 (2013).

- ⁶M. J. Mendes, E. Hernández, E. López, P. García-Linares, I. Ramiro, I. Artacho, E. Antolín, I. Tobías, A. Martí, and A. Luque, *Nanotechnology* **24**, 345402 (2013).
- ⁷H. Tan, R. Santbergen, A. H. Smets, and M. Zeman, *Nano Lett.* **12**, 4070 (2012).
- ⁸O. Isabella, S. Solntsev, D. Caratelli, and M. Zeman, *Prog. Photovoltaics* **21**, 94 (2013).
- ⁹S. Zanotto, M. Liscidini, and L. C. Andreani, *Opt. Express* **18**, 4260 (2010).
- ¹⁰A. Bozzola, M. Liscidini, and L. C. Andreani, *Opt. Express* **20**, A224 (2012).
- ¹¹C. Martella, D. Chiappe, P. Delli Veneri, L. Mercaldo, I. Usatii, and F. Buatier de Mongeot, *Nanotechnology* **24**, 225201 (2013).
- ¹²R. Peretti, G. Gomard, L. Lalouat, C. Seassal, and E. Drouard, *Phys. Rev. A* **88**, 053835 (2013).
- ¹³G. Gomard, R. Peretti, E. Drouard, X. Meng, and C. Seassal, *Opt. Express* **21**, A515 (2013).
- ¹⁴A. Abass, C. Trompoukis, S. Leyre, M. Burgelman, and B. Maes, *J. Appl. Phys.* **114**, 033101 (2013).
- ¹⁵M. Burresti, F. Pratesi, K. Vynck, M. Prasciolu, M. Tormen, and D. S. Wiersma, *Opt. Express* **21**, A268 (2013).
- ¹⁶F.-J. Haug, A. Naqavi, and C. Ballif, *J. Appl. Phys.* **112**, 024516 (2012).
- ¹⁷H. Shigetani, M. Fujita, Y. Tanaka, A. Oskooi, H. Ogawa, Y. Tsuda, and S. Noda, *Appl. Phys. Lett.* **101**, 161103 (2012).
- ¹⁸A. Bozzola, M. Liscidini, and L. C. Andreani, "Broadband light trapping with disordered photonic structures in thin-film silicon solar cells," *Prog. Photovoltaics* (published online).
- ¹⁹K. X. Wang, Z. Yu, V. Liu, Y. Cui, and S. Fan, *Nano Lett.* **12**, 1616 (2012).
- ²⁰S. Eyderman, S. John, and A. Deinega, *J. Appl. Phys.* **113**, 154315 (2013).
- ²¹E. R. Martins, J. Li, Y. Liu, V. Depauw, Z. Chen, J. Zhou, and T. F. Krauss, *Nat. Commun.* **4**, 2665 (2013).
- ²²M. Ernst and R. Brendel, *Phys. Status Solidi RRL* **8**, 235 (2014).
- ²³A. Ingenito, O. Isabella, and M. Zeman, *ACS Photon.* **1**, 270 (2014).
- ²⁴A. Deinega, S. Eyderman, and S. John, *J. Appl. Phys.* **113**, 224501 (2013).
- ²⁵O. Isabella, H. Sai, M. Kondo, and M. Zeman, "Full-wave optoelectrical modeling of optimized flattened light-scattering substrate for high efficiency thin-film silicon solar cells," *Prog. Photovoltaics* (published online).
- ²⁶M. G. Deceglie, V. E. Ferry, A. P. Alivisatos, and H. A. Atwater, *Nano Lett.* **12**, 2894 (2012).
- ²⁷G. Gomard, X. Meng, E. Drouard, K. El Hajjam, E. Gerelli, R. Peretti, A. Fave, R. Orobtcouk, M. Lemiti, and C. Seassal, *J. Opt.* **14**, 024011 (2012).
- ²⁸A. Ingenito, O. Isabella, S. Solntsev, and M. Zeman, *Sol. Energy Mater. Sol. Cells* **123**, 17 (2014).
- ²⁹M. Peters, M. Rüdiger, B. Bläsi, and W. Platzer, *Opt. Express* **18**, A584 (2010).
- ³⁰I. Simonsen, *Eur. Phys. J. Spec. Top.* **181**, 1 (2010).
- ³¹S. Fahr, T. Kirchartz, C. Rockstuhl, and F. Lederer, *Opt. Express* **19**, A865 (2011).
- ³²K. Jäger, M. Fischer, R. Van Swaaij, and M. Zeman, *J. Appl. Phys.* **111**, 083108 (2012).
- ³³K. Jäger, M. Fischer, R. A. van Swaaij, and M. Zeman, *Opt. Express* **21**, A656 (2013).
- ³⁴T. Lanz, B. Ruhstaller, C. Battaglia, and C. Ballif, *J. Appl. Phys.* **110**, 033111 (2011).
- ³⁵N. Sahraei, K. Forberich, S. Venkataraj, A. G. Aberle, and M. Peters, *Opt. Express* **22**, A53 (2014).
- ³⁶D. Dominé, F.-J. Haug, C. Battaglia, and C. Ballif, *J. Appl. Phys.* **107**, 044504 (2010).
- ³⁷S. Wiesendanger, M. Zilk, T. Pertsch, F. Lederer, and C. Rockstuhl, *Appl. Phys. Lett.* **103**, 131115 (2013).
- ³⁸J. Dore, D. Ong, S. Varlamov, R. Egan, and M. Green, *IEEE J. Photovoltaics* **4**, 33 (2014).
- ³⁹J. H. Petermann, D. Zielke, J. Schmidt, F. Haase, E. G. Rojas, and R. Brendel, *Prog. Photovoltaics* **20**, 1 (2012).
- ⁴⁰V. Depauw, Y. Qiu, K. Van Nieuwenhuysen, I. Gordon, and J. Poortmans, *Prog. Photovoltaics* **19**, 844 (2011).
- ⁴¹X. Meng, V. Depauw, G. Gomard, O. El Daif, C. Trompoukis, E. Drouard, C. Jamois, A. Fave, F. Dross, I. Gordon, and C. Seassal, *Opt. Express* **20**, A465 (2012).
- ⁴²C. Trompoukis, O. El Daif, V. Depauw, I. Gordon, and J. Poortmans, *Appl. Phys. Lett.* **101**, 103901 (2012).
- ⁴³H. Sai, K. Saito, N. Hozuki, and M. Kondo, *Appl. Phys. Lett.* **102**, 053509 (2013).
- ⁴⁴M. Boccard, C. Battaglia, S. Hanni, K. Soderstrom, J. Escarré, S. Nicolay, F. Meillaud, M. Despeisse, and C. Ballif, *Nano Lett.* **12**, 1344 (2012).
- ⁴⁵K. Söderström, G. Bugnon, F.-J. Haug, S. Nicolay, and C. Ballif, *Sol. Energy Mater. Sol. Cells* **101**, 193 (2012).
- ⁴⁶P. Kowalczewski, M. Liscidini, and L. C. Andreani, *Opt. Lett.* **37**, 4868 (2012).
- ⁴⁷J. Escarré, J. Bertomeu, J. Asensi, J. Andreu, V. Terrazoni-Daudrix, F.-J. Haug, and X. Niquille, in *Conference Record of the 2006 IEEE 4th World Conference on Photovoltaic Energy Conversion* (IEEE, 2006), Vol. 2, pp. 1556–1559.
- ⁴⁸D. Whittaker and I. Culshaw, *Phys. Rev. B* **60**, 2610 (1999).
- ⁴⁹M. Liscidini, D. Gerace, L. C. Andreani, and J. Sipe, *Phys. Rev. B* **77**, 035324 (2008).
- ⁵⁰See http://www.silvaco.com/products/tcad/device_simulation/atlas/atlas.html for "Silvaco Atlas."
- ⁵¹P. Kowalczewski, M. Liscidini, and L. C. Andreani, *Opt. Express* **21**, A808 (2013).
- ⁵²V. Freilikher, E. Kanziiper, and A. Maradudin, *Phys. Rep.* **288**, 127 (1997).
- ⁵³C. Rockstuhl, S. Fahr, K. Bittkau, T. Beckers, R. Carius, F.-J. Haug, T. Söderström, C. Ballif, and F. Lederer, *Opt. Express* **18**, A335 (2010).
- ⁵⁴E. D. Palik, *Handbook of Optical Constants of Solids* (Academic, Orlando, 1985).
- ⁵⁵See <http://rredc.nrel.gov/solar/spectra/am1.5/> for "Reference solar spectral irradiance: Air mass 1.5."
- ⁵⁶M. Taguchi, A. Yano, S. Tohoda, K. Matsuyama, Y. Nakamura, T. Nishiwaki, K. Fujita, and E. Maruyama, *IEEE J. Photovoltaics* **4**, 96 (2014).
- ⁵⁷J. Zhao, A. Wang, M. A. Green, and F. Ferrazza, *Appl. Phys. Lett.* **73**, 1991 (1998).
- ⁵⁸J. Dziewior and W. Schmid, *Appl. Phys. Lett.* **31**, 346 (1977).
- ⁵⁹A. Bozzola, P. Kowalczewski, and L. Andreani, *J. Appl. Phys.* **115**, 094501 (2014).
- ⁶⁰H. B. Li, R. H. Franken, J. K. Rath, and R. E. Schropp, *Sol. Energy Mater. Sol. Cells* **93**, 338 (2009).
- ⁶¹B. Hoex, S. Heil, E. Langereis, M. Van de Sanden, and W. Kessels, *Appl. Phys. Lett.* **89**, 042112 (2006).